



HAL
open science

In situ measurement of full adsorption isotherms by NMR

João Marreiros, Rodrigo de Oliveira-Silva, Paul Iacomi, Philip Llewellyn, Rob Ameloot, Dimitrios Sakellariou

► **To cite this version:**

João Marreiros, Rodrigo de Oliveira-Silva, Paul Iacomi, Philip Llewellyn, Rob Ameloot, et al.. In situ measurement of full adsorption isotherms by NMR. *Journal of the American Chemical Society*, 2021, 143 (22), pp.8249-8254. 10.1021/jacs.1c03716 . hal-03662675

HAL Id: hal-03662675

<https://hal.science/hal-03662675v1>

Submitted on 9 May 2022

HAL is a multi-disciplinary open access archive for the deposit and dissemination of scientific research documents, whether they are published or not. The documents may come from teaching and research institutions in France or abroad, or from public or private research centers.

L'archive ouverte pluridisciplinaire **HAL**, est destinée au dépôt et à la diffusion de documents scientifiques de niveau recherche, publiés ou non, émanant des établissements d'enseignement et de recherche français ou étrangers, des laboratoires publics ou privés.

In situ measurement of full adsorption isotherms by NMR

João Marreirosa‡, Rodrigo de Oliveira-Silvaa‡, Paul Iacomib, Philip L. Llewellynb,c, Rob Ameloota and Dimitrios Sakellarioua*.

acMACS, Department of Microbial and Molecular Systems (M²S), KU Leuven, 3001 Leuven, Belgium.

bAix-Marseille Univ., CNRS, MADIREL UMR 7246, 13397 Marseille, France.

c TOTAL SE, E&P, Centre Scientifique et Technique Jean Féger, 64000 Pau, France.

KEYWORDS porous materials, physisorption, MOFs, low-field NMR relaxometry.

ABSTRACT: Physisorption using gas or vapor probe molecules is the most common characterization technique for porous materials. The method provides textural information on the adsorbent as well as the affinity for a specific adsorbate, typically through equilibrium pressure measurements. Here, we demonstrate how low-field NMR can be used to measure full adsorption isotherms, and how by selectively measuring ¹H spins of the adsorbed probe molecules, rather than those in the vapor phase, this ‘NMR-relaxorption’ technique provides insights about local dynamics beyond what can be learned from physisorption alone. The potential of this double-barreled approach was illustrated for a set of microporous metal-organic frameworks (MOFs). For methanol adsorption in ZIF-8 the method identifies multiple guest molecules populations assigned to MeOH clusters in the pore center, MeOH bound at cage windows and to MeOH adsorption on defect sites. For UiO-66(Zr) the sequential pore filling is demonstrated and accurate pore topologies are directly obtained, and for MIL-53(Al) structural phase transitions are accurately detected and linked with two populations of dimeric chemical species localized to specific positions in the framework.

Porous solids with a high specific surface area exhibit unique physical and chemical properties and are crucial in catalytic¹ and separation processes.^{2–4} Typically, the ad-sorption characteristics of such materials are evaluated by recording their uptake of a probe molecule as a function of its partial pressure at a given temperature.⁵ While such physisorption methods are commonplace and established, the underlying adsorbent-adsorbate interactions are inferred from the macroscopic pressure-loading curves according to necessarily approximating models. Nuclear magnetic resonance (NMR) probes matter at the atomic level and can provide information inside these materials but its integration is not trivial. Early studies used electro-magnets to study NMR relaxation as a function of temperature.^{6–8} Modern day high-field NMR spectroscopy can offer a much more detailed picture, down to the atomic scale, by directly probing the adsorbed phase in terms of structure and dynamics. To date, however, mainly single-point adsorption high-field NMR experiments have been performed, since full isotherm measurements are non-trivial to implement on superconducting NMR instruments,^{9–13} or otherwise deviate from the ideal conditions set as industry standards for isotherm acquisition (e.g. using gravimetric techniques, imaging, etc.).^{14,15} Recent studies have attempted to circumvent these limitations with the use of low-field NMR for the study of sorbent materials. Nonetheless these remain limited to ex situ sample analysis and often require the use of intricate custom-made high-pressure gas dosing systems.^{18–20}

Herein, we showcase the integration of an ultra-compact low-field NMR device with a commercial physisorption instrument. Relaxometric measurements of adsorbed molecules are used to monitor and elucidate adsorption inter-actions and dynamics as a function of partial pressure. A small size homogeneous Halbach-like permanent magnet (0.3 T, 1200 cm³, 4 kg) and a solenoidal coil were used for polarizing, exciting and detecting the NMR signal. Their integration with the commercial sorption analyser was seamless due to the negligible stray magnetic field of the magnet. It is notoriously difficult to record signals from vapors, or gases by NMR because of their low spin density, which has given rise to the use of gas hyperpolarization techniques (CITE 16+17). In our case however, the concentration through adsorption in porous media, combined with a high-sensitivity multiple-pulse sequence, allow detection of the adsorbed guest phase. Approximately 20 mg of various adsorbents were loaded in a custom dead-end glass sample tube fully compatible with the commercial adsorption apparatus, so that no modifications are required to the activation and isotherm measurement protocol (Figure S1 in SI). The NMR measurements were performed simultaneously with the isotherm measurements, by averaging 32 Carr-Purcell-Meiboom-Gill^{21,22} (CPMG) scans every ~180 seconds. For all tested adsorbent-adsorbate combinations, natural-abundance ¹H NMR measurements under thermal polarisation and standard pressures gave a sufficiently high signal while also measuring longitudinal (T₁) and transverse (T₂) nuclear relaxation times. Non-adsorbed guest molecules were not detected by NMR due to their low ¹H spin density. The NMR signal intensity was obtained by integrating the first 10 Hahn echoes, corresponding to a signal duration of 2 ms. The inverse Laplace transform (ILT) was used to fit the data and extract relaxation time distributions. This mode of detection filters out NMR signals that have very short (< 200 μs) T₂ times. Although chemical shifts were not resolved because of the low magnetic field, different guest populations could be distinguished based on differences in T₁ and/or in T₂. Moreover, 2D correlation NMR experiments between T₁ and T₂ at specific partial pressures enabled to estimate the adsorbent-adsorbate interaction energy parameter (ϵ_{surf}).²³

Single-pore MOF – ZIF-8

The relaxorption technique was demonstrated for the physisorption of methanol (MeOH) in ZIF-8, a MOF consisting of Zn²⁺ ions and 2-methylimidazolate linkers.²⁴ The MeOH NMR signal as a function of partial pressure corresponds with both the adsorption isotherm (Figure 1a – white and red lines) and previously reported data.^{25–28} A previous computational study on this system predicted two sorption stages: initial trace adsorption on the pore walls, followed by adsorbate clustering in the center of the pore.²⁸ In excellent accordance, the NMR relaxation measurements show a two-stage process with a minimal signal at $p/p_0 < 0.15$, followed by a strong signal for partial pressures above 0.15. The low NMR signal intensity at low pressures can be attributed to the strong bonding of the small number of adsorbed molecules, resulting in a very short T₂, less than 100 μs, for accurate signal detection. Where the isotherm rises steeply ($0.15 < p/p_0 < 0.25$), increasingly longer T₂ values are observed. These changes correspond well to a shift of MeOH molecules from the pore wall sites towards the center of the pore.²⁸ At even higher partial pressures ($0.25 < p/p_0$; Qads > 9.6 mmol/g), T₂ remains constant for the majority of the adsorbed molecules (T₂ ~ 100 ms), but a low-intensity population with a shorter T₂ about 10 ms is also detectable, suggesting a small fraction of strongly adsorbed molecules besides those clustered in the pore center.

To better understand the different populations of adsorbed molecules at selected partial pressures, 2D T₁ – T₂ correlations were measured for longer periods of time in order to achieve a higher signal-to-noise

ratio (Figure S3; experimental details in SI). At a partial pressure of 0.125 (Figure 1a, red square), the 2D T1 – T2 NMR correlation map (Figure 1b) displays three resolved peaks, corresponding to individual populations of ^1H spins (A, B, and C). Population A is present throughout the isotherm, and its signal intensity grows at higher partial pressures, likely corresponding to hydrogen-bonded MeOH clusters in the pore center. Population B is dominant at low partial pressures and fades as more MeOH is adsorbed. Therefore, it is attributed to MeOH adsorbed at cage windows and pore walls.²⁸ Since the population C has the lowest signal intensity and shortest T2, it likely corresponds to adsorption on defect sites, especially given that the used synthesis method is prone to defect formation.^{29,30} The surface interaction parameter $e_{\text{surf}} = -T_2/T_1$, originally introduced by D'Agostino et al.,²³ is a quantitative estimator of the adsorbate–adsorbent interactions during adsorption. Applying this theory here, populations B and C have similar interaction strengths, in accordance with e_{surf} as indicated by their distance from the diagonal (Figure 1b).²³ Analysis of e_{surf} shows a weakening of the host-guest interactions with increased vapor loading (Figure S23).

While the low magnetic field prevents NMR identification of different adsorbates by chemical shift analysis, the different interaction strengths of ethanol (EtOH) and MeOH with ZIF-8 result in distinct T2 relaxation times (Figure 1c). This difference enabled uptake monitoring of each component from a MeOH/EtOH vapor mixture (see Figure S8). In contrast to MeOH, the stronger host-guest interactions for EtOH result in adsorption exclusively on the pore walls, without migration towards the center, leading to shorter T2 values. This strong confinement results in a different profile between the NMR intensity and the isotherm (Figure S7) since wall-bound molecules relax faster, leading to a partial loss of the NMR signal at low partial pressures and highlighting the underlying sorption mechanism.

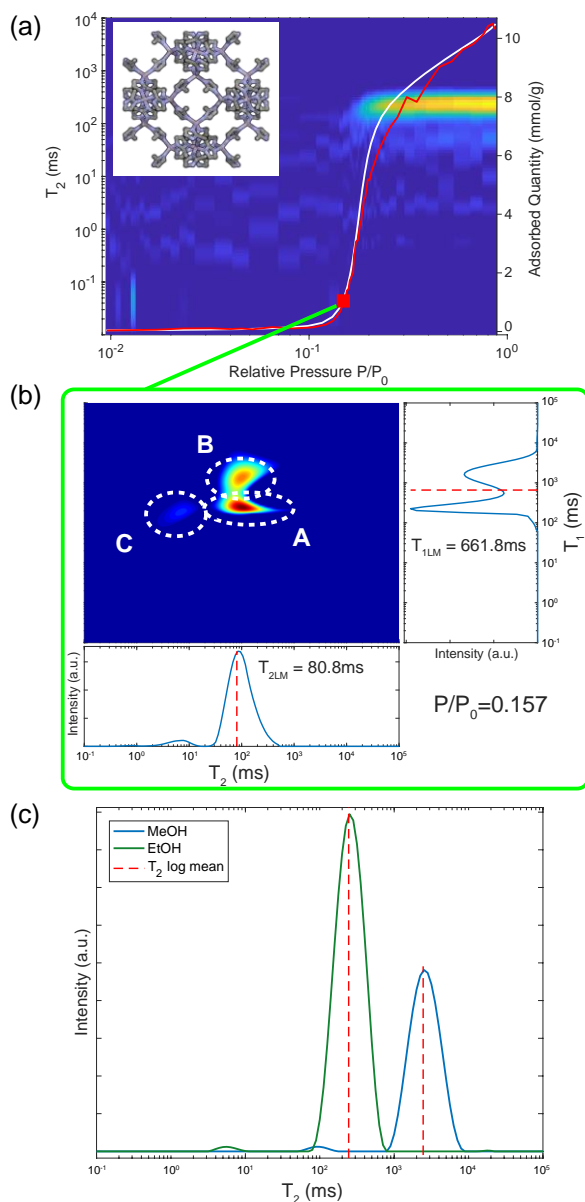


Figure 1 - Alcohol vapor adsorption on powdered ZIF-8 monitored by the NMR relaxation technique. a) The adsorption isotherm (white line) and the NMR signal intensity (red line) are shown as a function of partial pressure. A 2D graph of the T_2 relaxation time distribution (vertical axis) also as a function of the loading (same horizontal axis) is placed below these curves, for comparison. In the inset the porous structure of the ZIF-8 is represented. b) T_1 - T_2 correlation map for MeOH loading of 1.8 mmol/g ($p/p_0 = 0.157$). Three adsorbate populations are identified - A, B and C. c) T_2 relaxation time distributions for EtOH (green) and MeOH (blue) in ZIF-8 ($p/p_0 = 0.8$). The two curves show different average relaxation times leading to speciation.

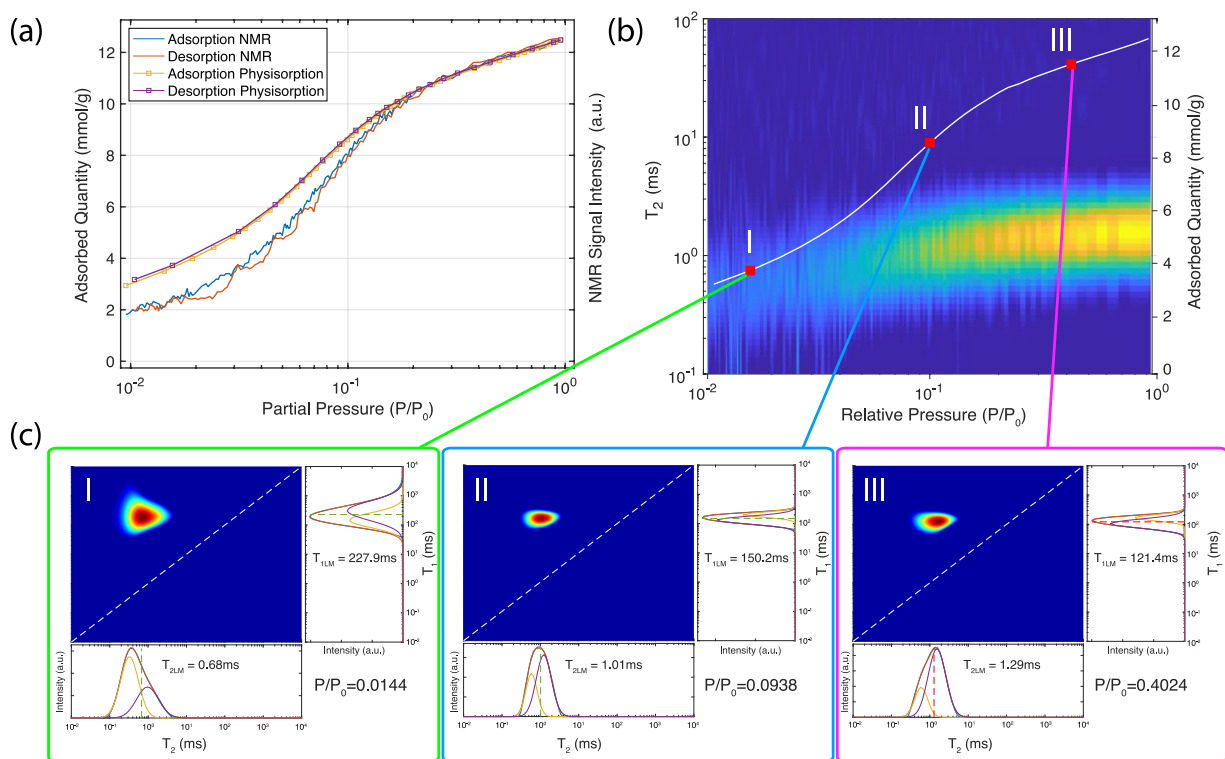


Figure 2 - Ethanol adsorption on powdered UiO-66(Zr). a) Superposition of the NMR signal intensity and the physisorption isotherm. b) Physisorption isotherm (white curve) superimposed with the T_2 distributions as a function of partial pressure. The red squares outline the loadings where T_1 - T_2 experiments were performed and their results are shown in c). The 1D projections of these 2D maps were deconvoluted in two components. The white dotted line correspond to the lines T_1/T_2 equal to 1 (diagonal).

Dual-pore MOF – UiO-66(Zr)

UiO-66(Zr), a dual-pore MOF built up of zirconium clusters and terephthalate linkers³¹ was also studied by relaxorption. As for ZIF-8, ethanol adsorption revealed a difference between the isotherm and the NMR signal intensity in the low-pressure region ($p/p_0 < 0.1$; Figure 2a, Figure S11). This difference is attributed to strong EtOH adsorption expected in the low partial pressure regime ($0.05 < p/p_0$) due to hydrogen bonding with the inorganic clusters.¹² This hypothesis is fully validated by the short average (about 300 μ s) transverse NMR relaxation times. At the lowest EtOH loading (2.94 mmol/g; $p/p_0 = 0.0095$), an estimated 1.2 mmol/g of alcohol are cluster-bound and thus beyond the limits of NMR detection (Figure 2a, Figure S11). NMR sensitivity is progressively restored as more EtOH is adsorbed ($Q_{ads} > 2.94$ mmol/g; $0.0095 < p/p_0$), with an increase in T_2 relaxation times, likely due to competing guest-guest interactions. This hypothesis is supported by the increasing isosteric enthalpy of adsorption as a function of loading (Figure S14). As a result, at partial pressures above 0.2, the NMR signal intensity and physisorption data correspond well (Figure 2a).

2D T₁ – T₂ correlation experiments reveal a bimodal T₂ distribution, as might be expected for the dual-pore network of UiO-66(Zr) (Figures 2c, S10-S13). At highest loading (Q_{ads} = 12.40 mmol/g; p/p₀ = 0.90) the deconvoluted and integrated T₂ signals designated T₂T (tetrahedral pores, 38%) and T₂O (octahedral pores, 62%), corresponded well to the volume fractions of the tetrahedral and octahedral pores in UiO-66(Zr) (SI section I-b; VT = 40% and VO = 60%). The changes to T₂T and T₂O, over the course of the isotherm, reveal partial occupancy of both tetrahedral and octahedral pores, with preferential loading of the former at low pressures (Q_{ads} = 4.46 mmol/g; p/p₀ = 0.0242). Further EtOH adsorption results in the saturation of the tetrahedral pore, followed by filling of the octahedral pore. Prior studies on the adsorption of CO₂ in UiO-66(Zr) found a similar pore loading preference.^{32,33} Furthermore, an inverse linear relation between the quantity of adsorbed EtOH and esurf is observed (Figure S14). Similarly as for ZIF-8, increased loading favors guest-guest interactions which compete with the framework-vapor interactions and this leads to a reduction of esurf. This hypothesis is further confirmed by the increase in isosteric enthalpy of adsorption as a function of loading.

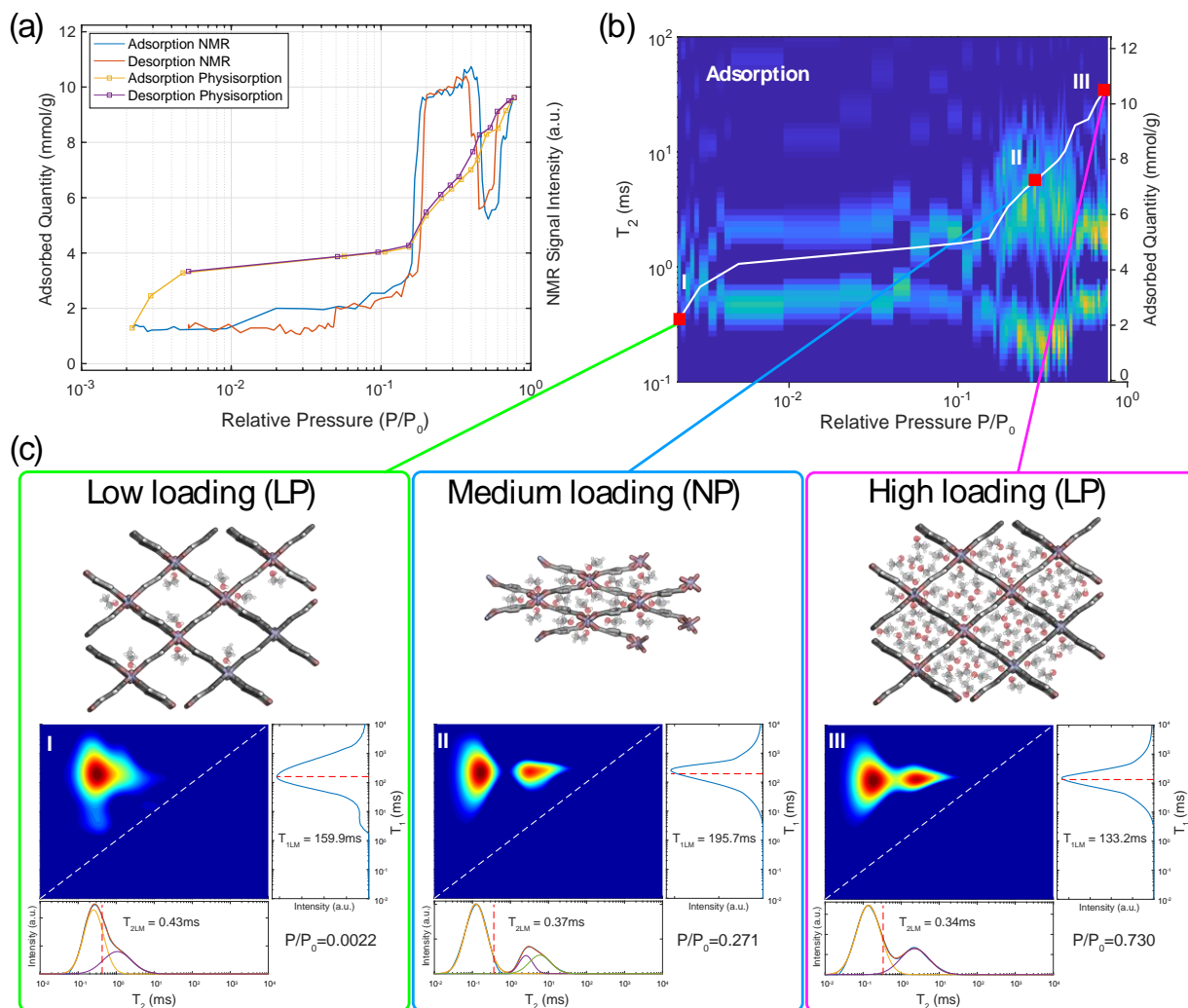


Figure 3 - Ethanol adsorption on powdered MIL-53(Al). a) Superposition of the NMR signal and physisorption isotherms. Low field NMR was able to identify the conformational transitions, from LP (I) to NP (II) and again to LP(III) by the changes in the intensity of signal due to the loading of EtOH molecules.

b) Evolution of the transverse relaxation times (T_2) as a function of the loading. The physisorption isotherm (white line) is superimposed with the T_2 distributions. The red squares are the loadings where the T_1 - T_2 2D NMR experiments were performed. c) Three T_1 - T_2 correlation maps for the different conformational states I, II, and III. The evolution of guest populations is observed with the loading as well as changes in T_1 and T_2 . The white dotted lines correspond to the lines T_1/T_2 equal to 1 (diagonal).

Flexible MOF – MIL-53(Al)

Structural flexibility is a guest-induced response exhibited by the MIL-53 family of materials, which exhibit structural phase transitions as a function of pore occupancy, also known as “breathing”.^{34–36} During EtOH adsorption, MIL-53 undergoes a contraction from a large-pore (LP) to a narrow-pore (NP) state, followed by gradual re-opening at increasing pressures.³⁵ The EtOH isotherm and NMR intensity reveal unprecedented joint information. The NMR signal shows discontinuities and abrupt intensity fluctuations where structural transitions occur due to changes in the dynamics of the guest molecules (Figure 3a). In the initial LP form, T_2 relaxation times of 0.5 and 1 ms are observed. With increasing loading, the phase transition to the NP configuration shortens the former relaxation time to 0.2 ms, while increasing the latter to 3 ms. Upon re-opening of the pores, T_2 values close to the initial value are measured – small T_2 deviations arise from the fact the final LP state does not perfectly match the initial LP state of MIL-53(Al) at the beginning of the isotherm. Changes in molecular dynamics impact the relaxation times and explain the differences in NMR signal intensity in Figure 3a, in line with water adsorption in MIL-53(Cr).³³

2D T_1 - T_2 maps at specific EtOH loadings confirm the existence of loading-dependent bimodal T_2 distributions correlated to a single T_1 , whose value fluctuates also as function of guest loading (Figure 3c). Deconvolution of the T_2 relaxation times reveals two (and possibly three at higher loading) guest populations, ascribed to the different guest-host coordination modes originally reported by Bourelly et al.³¹ These T_2 components are likely matched to EtOH monomer coordination at Al(OH) cluster level (shorter T_2 values), as well as dimer and trimer coordinations (longer T_2 values ~ 10 ms). The average surface interaction parameter e_{surf} changes abruptly as a function of guest loading, contrary to the continuously declining profiles observed for UiO-66(Zr) and ZIF-8 (Figure S23). Non-breathing sorbents such as ZIF-8 and UiO-66(Zr), show a continuous lowering in e_{surf} with increased guest loading. By comparison, flexible materials display more complex e_{surf} profiles with considerable fluctuations of this parameter, either $\Delta e_{surf} > 0$ or $\Delta e_{surf} < 0$ corresponding to a phase transition or guest loading, respectively. In correspondence with crystallographic data, Δe_{surf} from NMR measurements may be used as a descriptor for the MIL-53(Al) phase transition, offering a clear distinction between strict pore loading ($\Delta e_{surf} < 0$), and structural transformations ($\Delta e_{surf} > 0$).

Conclusion

Integration of physisorption and NMR relaxometry for in situ measurements, dubbed as “NMR-Relaxorption”, was demonstrated on three case-studies of prototypical microporous materials. Even though this technology is at an early stage, it already offered complementary insights into host-guest, guest-guest interactions, i.e. pore filling (UiO-66) and structural heterogeneity (ZIF-8), and host/guest dynamics, i.e. host phase transition (MIL-53(Al)). While the NMR signal sensitivity remains one of the main

obstacles of this technique, several options exist to overcome it, including the use of stronger magnetic fields, cryo-cooled detection, as well as extraneous highly polarized sources of atoms or molecules, which may allow the detection of physisorbed monolayers and finer details in future developments. Detection of species having very short T₂ times, as well as determination of isotropic chemical shifts inside heterogeneous/solid materials remain the core challenge, but the use of strong radiofrequency pulses and low magnetic fields might enhance alternative options for averaging anisotropy such as magic angle field spinning.^{39,40} Ultimately, this methodology has the potential to become a low-cost general technique for the analysis of other material classes (e.g. zeolites, carbons, silicas, biopolymers, amongst others) for which structural heterogeneity, host/guest mobility, paramagnetism or phase transitions warrant further research.

ASSOCIATED CONTENT

Supporting Information. Full description of the experimental details including XRD patterns, TGA curves, sorption isotherms, NMR results and all modelling results. This material is available free of charge via the Internet at <http://pubs.acs.org>.

AUTHOR INFORMATION

Corresponding Author

* Prof. Dimitrios Sakellariou (dimitrios.sakellariou@kuleuven.be)

Present Addresses

†Dr. Paul Iacomì - ICGM, CNRS / Université de Montpellier, France.

Author Contributions

The manuscript was written through contributions of all authors. / All authors have given approval to the final version of the manuscript. / ‡These authors contributed equally.

Funding Sources

This project was supported by the KU Leuven Starting Grant and by the Research Foundation Flanders (FWO) under Grant PorMedNMR – n° GOD5419N.

ACKNOWLEDGMENT

DS is grateful to the CEA for many years of continuous support. The authors would like to thank Prof. D. De Vos for stimulating discussions and access to the 3Flex sorption instrument, and Prof. J. Karger for stimulating discussions and useful literature references, and M. S. Usé for help with the assembling the PID temperature controller.

ABBREVIATIONS

NMR, nuclear magnetic resonance; p/p₀, partial pressure; Q_{ads}, quantity adsorbed; NP, narrow pore; LP, large pore.

REFERENCES

- (1) Nguyen, H. L.; Vu, T. T.; Nguyen, D.-K.; Trickett, C. A.; Doan, T. L. H.; Diercks, C. S.; Nguyen, V. Q.; Cordova, K. E. A Complex Metal-Organic Framework Catalyst for Microwave-Assisted Radical Polymerization. *Commun Chem* 2018, 1 (1), 70. <https://doi.org/10.1038/s42004-018-0071-6>.
- (2) Wu, Y.; Yuan, D.; He, D.; Xing, J.; Zeng, S.; Xu, S.; Xu, Y.; Liu, Z. Decorated Traditional Zeolites with Subunits of Metal-Organic Frameworks for CH₄/N₂ Separation. *An-gew. Chem. Int. Ed.* 2019, 58 (30), 10241–10244. <https://doi.org/10.1002/anie.201905014>.
- (3) Lin, R.-B.; Xiang, S.; Zhou, W.; Chen, B. Microporous Metal-Organic Framework Materials for Gas Separation. *Chem* 2019, S2451929419304668. <https://doi.org/10.1016/j.chempr.2019.10.012>.
- (4) Iacomì, P.; Formalik, F.; Marreiros, J.; Shang, J.; Rogacka, J.; Mohmeyer, A.; Behrens, P.; Ameloot, R.; Kuchta, B.; Llewellyn, P. L. Role of Structural Defects in the Adsorption and Separation of C₃ Hydrocarbons in Zr-Fumarate-MOF (MOF-801). *Chem. Mater.* 2019, 31 (20), 8413–8423. <https://doi.org/10.1021/acs.chemmater.9b02322>.
- (5) Thommes, M.; Kaneko, K.; Neimark, A. V.; Olivier, J. P.; Rodriguez-Reinoso, F.; Rouquerol, J.; Sing, K. S. W. Physisorption of Gases, with Special Reference to the Evaluation of Surface Area and Pore Size Distribution (IUPAC Technical Report). *Pure and Applied Chemistry* 2015, 87 (9–10), 1051–1069. <https://doi.org/10.1515/pac-2014-1117>.
- (6) Pfeifer, H. Nuclear Magnetic Resonance and Relaxation of Molecules Adsorbed on Solids. In *NMR Basic Principles and Progress / NMR Grundlagen und Fortschritte*; Diehl, P., Fluck, E., Kosfeld, R., Eds.; Springer Berlin Heidelberg: Berlin, Heidelberg, 1972; pp 53–153. https://doi.org/10.1007/978-3-642-65312-4_2.
- (7) Pfeifer, H. Surface Phenomena Investigated by Nuclear Magnetic Resonance. *Physics Reports* 1976, 26 (7), 293–338. [https://doi.org/10.1016/0370-1573\(76\)90021-1](https://doi.org/10.1016/0370-1573(76)90021-1).
- (8) Watanabe, M.; Itō, T. Magnetic Resonance Studies of Hydrogen Adsorbed on Zinc Oxide. Proton NMR of Chemisorbed Hydrogen and Molecular Hydrogen Adsorbed Ionically. *Jpn. J. Appl. Phys.* 1980, 19 (10), 1863–1872. <https://doi.org/10.1143/JJAP.19.1863>.
- (9) Berens, S.; Hillman, F.; Jeong, H.-K.; Vasenkov, S. Self-Diffusion of Pure and Mixed Gases in Mixed-Linker Zeolitic Imidazolate Framework-7-8 by High Field Diffusion NMR. *Microporous and Mesoporous Materials* 2019, 288, 109603. <https://doi.org/10.1016/j.micromeso.2019.109603>.
- (10) Berens, S.; Chmelik, C.; Hillman, F.; Kärger, J.; Jeong, H.-K.; Vasenkov, S. Ethane Diffusion in Mixed Linker Zeolitic Imidazolate Framework-7-8 by Pulsed Field Gradient NMR in Combination with Single Crystal IR Microscopy. *Physical Chemistry Chemical Physics* 2018, 20 (37), 23967–23975. <https://doi.org/10.1039/C8CP04889D>.
- (11) Thoma, R.; Kärger, J.; de Sousa Amadeu, N.; Nießing, S.; Janiak, C. Assessing Guest-Molecule Diffusion in Heterogeneous Powder Samples of Metal-Organic Frameworks through Pulsed-Field-Gradient (PFG) NMR Spectroscopy. *Chemistry - A European Journal* 2017, 23 (53), 13000–13005. <https://doi.org/10.1002/chem.201702586>.

- (12) Nandy, A.; Forse, A. C.; Witherspoon, V. J.; Reimer, J. A. NMR Spectroscopy Reveals Adsorbate Binding Sites in the Metal–Organic Framework UiO-66(Zr). *J. Phys. Chem. C* 2018, 122 (15), 8295–8305. <https://doi.org/10.1021/acs.jpcc.7b12628>.
- (13) An, Y.; Kleinhammes, A.; Doyle, P.; Chen, E.-Y.; Song, Y.; Morris, A. J.; Gibbons, B.; Cai, M.; Johnson, J. K.; Shukla, P. B.; Vo, M. N.; Wei, X.; Wilmer, C. E.; Ruffley, J. P.; Huang, L.; Tovar, T. M.; Mahle, J. J.; Karwacki, C. J.; Wu, Y. In Situ Nuclear Magnetic Resonance Investigation of Molecular Adsorption and Kinetics in Metal–Organic Framework UiO-66. *J. Phys. Chem. Lett.* 2021, 12 (2), 892–899. <https://doi.org/10.1021/acs.jpcllett.0c03504>.
- (14) Beyea, S. D.; Caprihan, A.; Clewett, C. F. M.; Glass, S. J. Spatially Resolved Adsorption Isotherms of Thermally Polarized Perfluorinated Gases in Yttria-Stabilized Tetragonal-Zirconia Polycrystal Ceramic Materials with NMR Imaging. *Appl. Magn. Reson.* 2002, 22 (2), 175–186. <https://doi.org/10.1007/BF03166101>.
- (15) Leisen, J.; W. Beckham, H.; Benham, M. Sorption Isotherm Measurements by NMR. *Solid State Nuclear Magnetic Resonance* 2002, 22 (2–3), 409–422. <https://doi.org/10.1006/snmr.2002.0069>.
- (16) Front Matter. In *New Developments in NMR*; Jackowski, K., Jaszunski, M., Eds.; Royal Society of Chemistry: Cambridge, 2016; pp P001–P004. <https://doi.org/10.1039/9781782623816-FP001>.
- (17) Barskiy, D. A.; Coffey, A. M.; Nikolaou, P.; Mikhaylov, D. M.; Goodson, B. M.; Branca, R. T.; Lu, G. J.; Shapiro, M. G.; Telkki, V.-V.; Zhivonitko, V. V.; Koptug, I. V.; Salnikov, O. G.; Kovtunov, K. V.; Bukhtiyarov, V. I.; Rosen, M. S.; Barlow, M. J.; Safavi, S.; Hall, I. P.; Schröder, L.; Chekmenev, E. Y. NMR Hyperpolarization Techniques of Gases. *Chem. Eur. J.* 2017, 23 (4), 725–751. <https://doi.org/10.1002/chem.201603884>.
- (18) Horch, C.; Schlayer, S.; Stallmach, F. High-Pressure Low-Field ^1H NMR Relaxometry in Nanoporous Materials. *Journal of Magnetic Resonance* 2014, 240, 24–33. <https://doi.org/10.1016/j.jmr.2014.01.002>.
- (19) Stallmach, F.; Pusch, A.-K.; Splith, T.; Horch, C.; Merker, S. NMR Relaxation and Diffusion Studies of Methane and Carbon Dioxide in Nanoporous ZIF-8 and ZSM-58. *Microporous and Mesoporous Materials* 2015, 205, 36–39. <https://doi.org/10.1016/j.micromeso.2014.08.034>.
- (20) Chen, J. J.; Mason, J. A.; Bloch, E. D.; Gygi, D.; Long, J. R.; Reimer, J. A. NMR Relaxation and Exchange in Metal–Organic Frameworks for Surface Area Screening. *Microporous and Mesoporous Materials* 2015, 205, 65–69. <https://doi.org/10.1016/j.micromeso.2014.07.037>.
- (21) Carr, H. Y.; Purcell, E. M. Effects of Diffusion on Free Precession in Nuclear Magnetic Resonance Experiments. *Phys. Rev.* 1954, 94 (3), 630–638. <https://doi.org/10.1103/PhysRev.94.630>.
- (22) Meiboom, S.; Gill, D. Modified Spin-Echo Method for Measuring Nuclear Relaxation Times. *Review of Scientific Instruments* 1958, 29 (8), 688–691. <https://doi.org/10.1063/1.1716296>.
- (23) D’Agostino, C.; Mitchell, J.; Mantle, M. D.; Gladden, L. F. Interpretation of NMR Relaxation as a Tool for Characterizing the Adsorption Strength of Liquids inside Porous Materials. *Chem. Eur. J.* 2014, 20 (40), 13009–13015. <https://doi.org/10.1002/chem.201403139>.

- (24) Park, K. S.; Ni, Z.; Côté, A. P.; Choi, J. Y.; Huang, R.; Uribe-Romo, F. J.; Chae, H. K.; O’Keeffe, M.; Yaghi, O. M. Exceptional Chemical and Thermal Stability of Zeolitic Imidazolate Frameworks. *Proceedings of the National Academy of Sciences* 2006, 103 (27), 10186–10191.
- (25) Gee, J. A.; Chung, J.; Nair, S.; Sholl, D. S. Adsorption and Diffusion of Small Alcohols in Zeolitic Imidazolate Frameworks ZIF-8 and ZIF-90. *J. Phys. Chem. C* 2013, 117 (6), 3169–3176. <https://doi.org/10.1021/jp312489w>.
- (26) Zhang, K.; Lively, R. P.; Dose, M. E.; Brown, A. J.; Zhang, C.; Chung, J.; Nair, S.; Koros, W. J.; Chance, R. R. Alcohol and Water Adsorption in Zeolitic Imidazolate Frameworks. *Chemical Communications* 2013, 49 (31), 3245. <https://doi.org/10.1039/c3cc39116g>.
- (27) Marreiros, J.; Van Dommelen, L.; Fleury, G.; Oliveira-Silva, R.; Stassin, T.; Iacomini, P.; Furukawa, S.; Sakellariou, D.; Llewellyn, P. L.; Roefsaers, M.; Ameloot, R. Vapor-Phase Linker Exchange of the Metal–Organic Framework ZIF-8: A Solvent-Free Approach to Post-synthetic Modification. *Angew. Chem. Int. Ed.* 2019, 58 (51), 18471–18475. <https://doi.org/10.1002/anie.201912088>.
- (28) Zhang, K.; Zhang, L.; Jiang, J. Adsorption of C 1 –C 4 Alcohols in Zeolitic Imidazolate Framework-8: Effects of Force Fields, Atomic Charges, and Framework Flexibility. *J. Phys. Chem. C* 2013, 117 (48), 25628–25635. <https://doi.org/10.1021/jp409869c>.
- (29) Abanades Lazaro, I.; Wells, C.; Forgan, R. S. Multivariate Modulation of the Zr MOF UiO-66 for Defect-Controlled Multimodal Anticancer Drug Delivery. *Angew. Chem. Int. Ed.* 2020. <https://doi.org/10.1002/anie.201915848>.
- (30) Vermoortele, F.; Bueken, B.; Le Bars, G.; Van de Voorde, B.; Vandichel, M.; Houthoofd, K.; Vimont, A.; Daturi, M.; Waroquier, M.; Van Speybroeck, V.; Kirschhock, C.; De Vos, D. E. Synthesis Modulation as a Tool To Increase the Catalytic Activity of Metal–Organic Frameworks: The Unique Case of UiO-66(Zr). *Journal of the American Chemical Society* 2013, 135 (31), 11465–11468. <https://doi.org/10.1021/ja405078u>.
- (31) Cavka, J. H.; Jakobsen, S.; Olsbye, U.; Guillou, N.; Lamberti, C.; Bordiga, S.; Lillerud, K. P. A New Zirconium Inorganic Building Brick Forming Metal Organic Frameworks with Exceptional Stability. *J. Am. Chem. Soc.* 2008, 130 (42), 13850–13851. <https://doi.org/10.1021/ja8057953>.
- (32) Grissom, T. G.; Driscoll, D. M.; Troya, D.; Sapienza, N. S.; Usov, P. M.; Morris, A. J.; Morris, J. R. Molecular-Level Insight into CO₂ Adsorption on the Zirconium-Based Metal–Organic Framework, UiO-66: A Combined Spectroscopic and Computational Approach. *J. Phys. Chem. C* 2019, 8.
- (33) Wiersum, A. D.; Soubeyrand-Lenoir, E.; Yang, Q.; Moulin, B.; Guillerm, V.; Yahia, M. B.; Bourrelly, S.; Vimont, A.; Miller, S.; Vagner, C.; Daturi, M.; Clet, G.; Serre, C.; Maurin, G.; Llewellyn, P. L. An Evaluation of UiO-66 for Gas-Based Applications. *Chemistry - An Asian Journal* 2011, 6 (12), 3270–3280. <https://doi.org/10.1002/asia.201100201>.
- (34) Serre, C.; Millange, F.; Thouvenot, C.; Noguès, M.; Marsolier, G.; Louër, D.; Férey, G. Very Large Breathing Effect in the First Nanoporous Chromium(III)-Based Solids: MIL-53 or Cr III (OH)-{O 2 C–C 6 H 4 –CO 2 }-x ·H 2 O y . *J. Am. Chem. Soc.* 2002, 124 (45), 13519–13526. <https://doi.org/10.1021/ja0276974>.

- (35) Millange, F.; Guillou, N.; Walton, R. I.; Grenèche, J.-M.; Margiolaki, I.; Férey, G. Effect of the Nature of the Metal on the Breathing Steps in MOFs with Dynamic Frameworks. *Chem. Commun.* 2008, No. 39, 4732. <https://doi.org/10.1039/b809419e>.
- (36) Weser, O.; Veryazov, V. In Search of the Reason for the Breathing Effect of MIL53 Metal-Organic Framework: An Ab Initio Multiconfigurational Study. *Front. Chem.* 2017, 5, 111. <https://doi.org/10.3389/fchem.2017.00111>.
- (37) Bourrelly, S.; Moulin, B.; Rivera, A.; Maurin, G.; Devautour-Vinot, S.; Serre, C.; Devic, T.; Horcajada, P.; Vimont, A.; Clet, G.; Daturi, M.; Lavalley, J.-C.; Loera-Serna, S.; Denoyel, R.; Llewellyn, P. L.; Férey, G. Explanation of the Adsorption of Polar Vapors in the Highly Flexible Metal Organic Framework MIL-53(Cr). *Journal of the American Chemical Society* 2010, 132 (27), 9488–9498. <https://doi.org/10.1021/ja1023282>.
- (38) Salles, F.; Bourrelly, S.; Jobic, H.; Devic, T.; Guillerm, V.; Llewellyn, P.; Serre, C.; Férey, G.; Maurin, G. Molecular Insight into the Adsorption and Diffusion of Water in the Versatile Hydrophilic/Hydrophobic Flexible MIL-53(Cr) MOF. *The Journal of Physical Chemistry C* 2011, 115 (21), 10764–10776. <https://doi.org/10.1021/jp202147m>.
- (39) Andrew, E. R.; Eades, R. G. Possibilities for High-Resolution Nuclear Magnetic Resonance Spectra of Crystals. *Discuss. Faraday Soc.* 1962, 34, 38. <https://doi.org/10.1039/df9623400038>.
- (40) Sakellariou, D.; Hugon, C.; Guiga, A.; Aubert, G.; Cazaux, S.; Hardy, P. Permanent Magnet Assembly Producing a Strong Tilted Homogeneous Magnetic Field: Towards Magic Angle Field Spinning NMR and MRI: Towards Magic Angle Field Spinning. *Magn. Reson. Chem.* 2010, 48 (12), 903–908. <https://doi.org/10.1002/mrc.2683>.